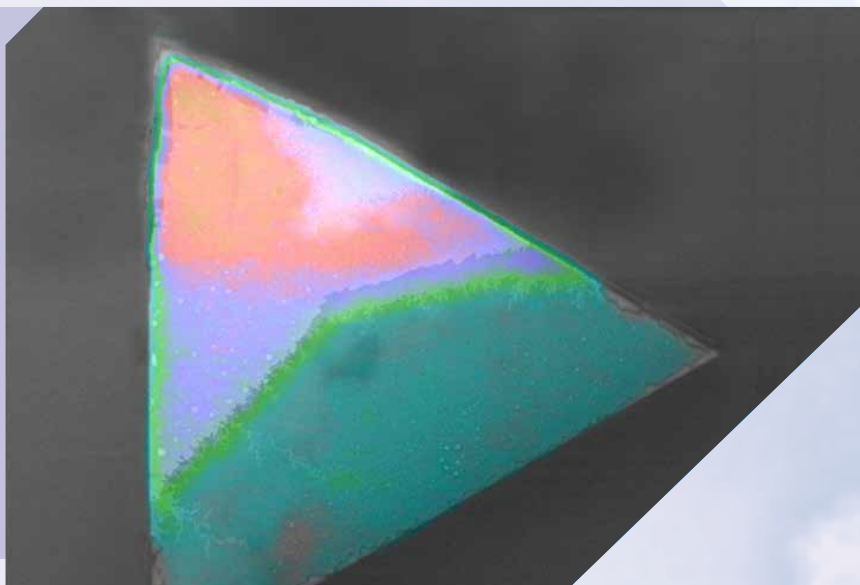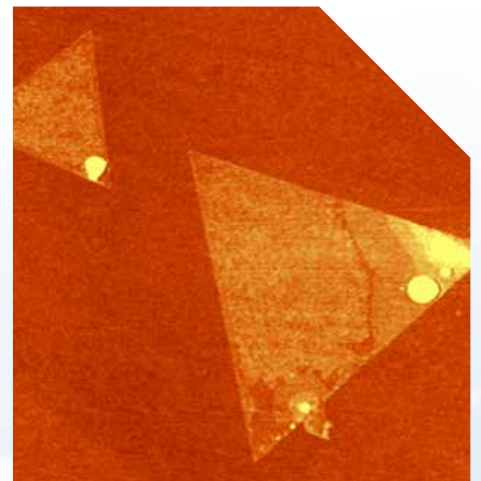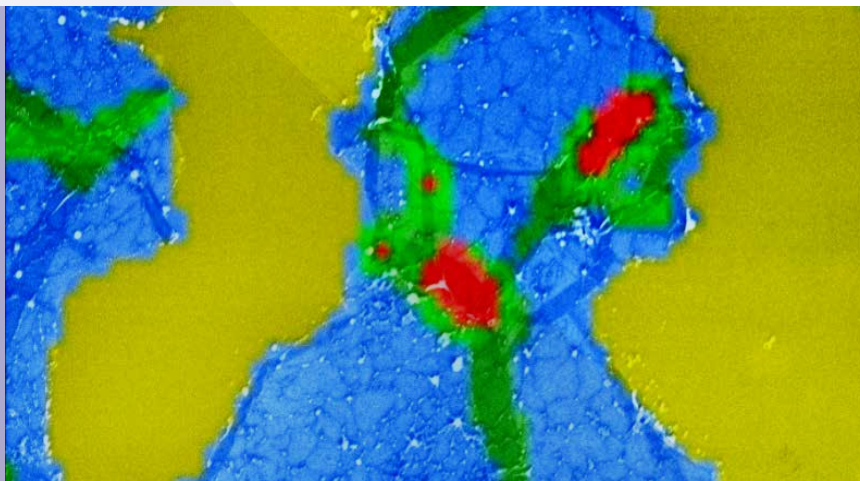# Correlative Confocal Raman Microscopy for 2D Materials Investigation

The Raman principle

The Raman effect is based on the inelastic scattering of light by the molecules of gaseous, liquid or solid materials. The interaction of a molecule with photons causes vibrations of its chemical bonds, leading to specific energy shifts in the scattered light. Thus, any given chemical compound produces a particular Raman spectrum when excited and can be easily identified by this individual "fingerprint."

Raman spectroscopy is a well-established, label-free and non-destructive method for analyzing the molecular composition of a sample.

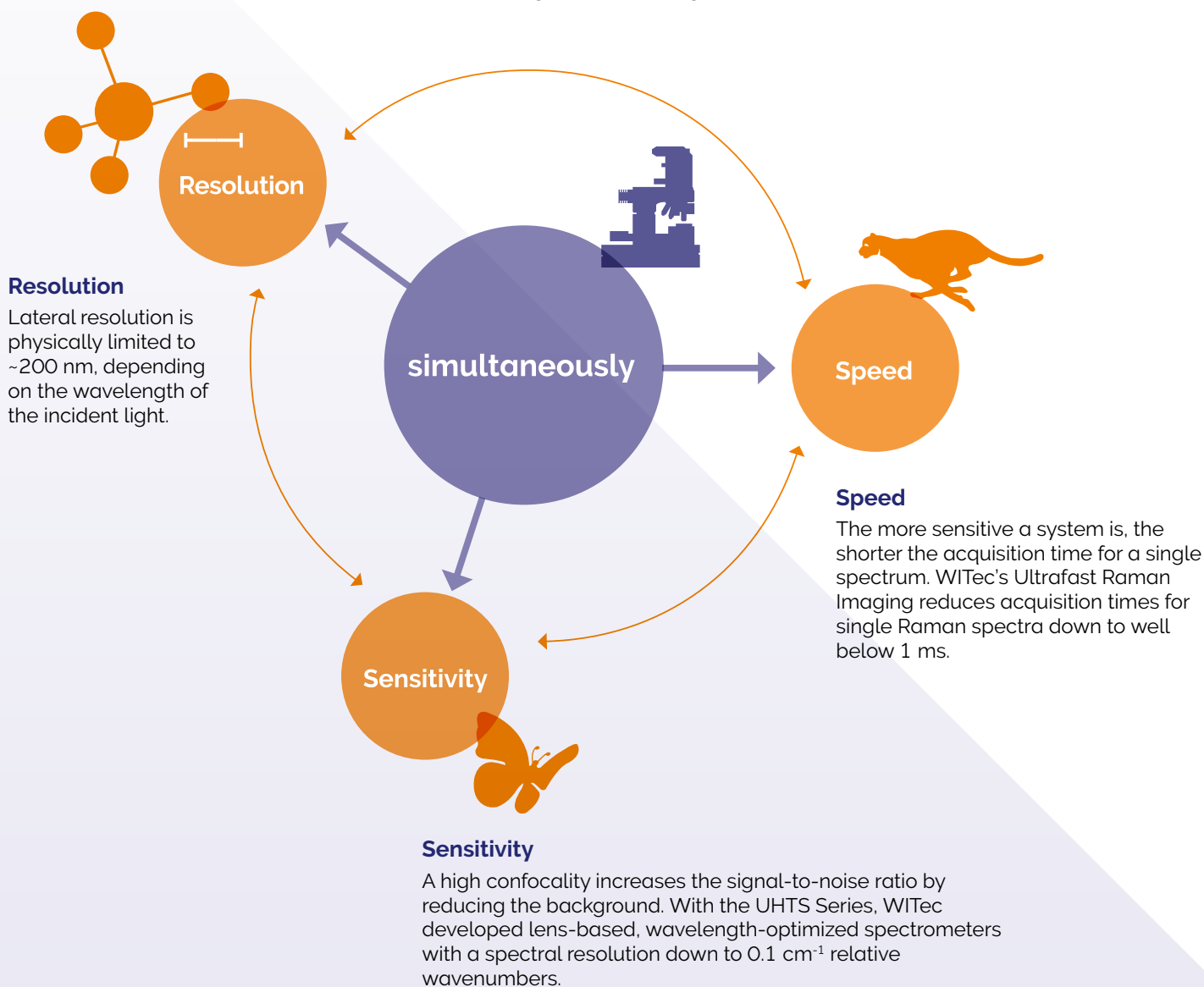$h\upsilon_0$ $h(\upsilon_0 \pm \upsilon)$
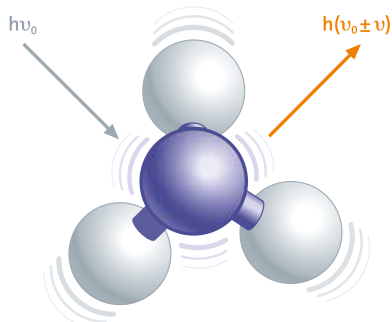
Raman imaging

In Raman imaging, a confocal microscope is combined with a spectrometer and a Raman spectrum is recorded at every image pixel. The resulting Raman image visualizes the distribution of the sample's compounds. Due to the high confocality of WITec Raman systems, volume scans and 3D images can also be generated.

No need for compromises

The Raman effect is extremely weak, so every Raman photon is important for imaging. Therefore WITec Raman imaging systems combine an exceptionally sensitive confocal microscope with an ultra-high throughput spectrometer (UHTS). Precise adjustment of all optical and mechanical elements guarantees the highest resolution, outstanding speed and extraordinary sensitivity – simultaneously!

This optimization allows the detection of Raman signals of even weak Raman scatterers and extremely low material concentrations or volumes with the lowest excitation energy levels. This is an unrivaled advantage of WITec systems.

Resolution

simultaneously

Speed

Sensitivity

Resolution

Lateral resolution is physically limited to ~200 nm, depending on the wavelength of the incident light.

Speed

The more sensitive a system is, the shorter the acquisition time for a single spectrum. WITec's Ultrafast Raman Imaging reduces acquisition times for single Raman spectra down to well below 1 ms.

Sensitivity

A high confocality increases the signal-to-noise ratio by reducing the background. With the UHTS Series, WITec developed lens-based, wavelength-optimized spectrometers with a spectral resolution down to 0.1 cm^{-1} relative wavenumbers.

Analyses of 2D materials with correlative Raman microscopy

The mechanical isolation of single-layer graphene with the help of adhesive tape in 2004 kicked off the rapid growth in research on materials consisting of only one or a few layers of atoms, defined as 2D materials. Different from bulk matter, they display interesting semiconducting characteristics that inspired an extensive exploration of their structural, electronic and optical properties. While graphene is still the most prominent example of a single-layered semiconducting material, other 2D materials such as transition metal dichalcogenides (TMDs or TMDCs) and black phosphorus also possess size-able bandgaps. In this application note we will describe both confocal Raman microscopy as a stand-alone technique and correlative Raman microscopy for the comprehensive investigation of 2D materials.

Confocal Raman imaging is an ideal method for studying 2D thin films, revealing their molecular characteristics through a non-destructive and fast procedure. It is used to discern the orientation of their layers and to investigate defects, strain and functionalization, as their Raman properties are determined by molecular bonds, relative orientation and number of layers. Their morphological details can be visualized with other high-resolution microscopy methods such as Scanning Electron Microscopy (SEM). By correlating the information of both approaches, 2D materials can be even more thoroughly analyzed.

WITec has developed microscopes that integrate confocal Raman imaging and optionally Atomic Force Microscopy (AFM), Scanning Near-field Optical Microscopy (SNOM) or SEM into one instrument for highly sensitive and efficient correlative microscopy.

Correlative topography and Raman measurements

RISE Microscopy is the combination of confocal Raman Imaging and Scanning Electron Microscopy (SEM). It incorporates the sensitivity of the non-destructive, spectroscopic Raman technique along with the high resolution of electron microscopy.

In Figure 1 the SEM (A) and RISE (C) images of a CVD-grown graphene sheet deposited on a Si/SiO$_2$ substrate are presented. Layer numbers were deduced from the Raman spectra (Figure 1B). The colors used represent a single layer (blue, dark green) with different grades of defects and more than one layer (light green, red). The RISE image highlights the large amount of defects in the blue area, in good agreement with the high-resolution SEM image.
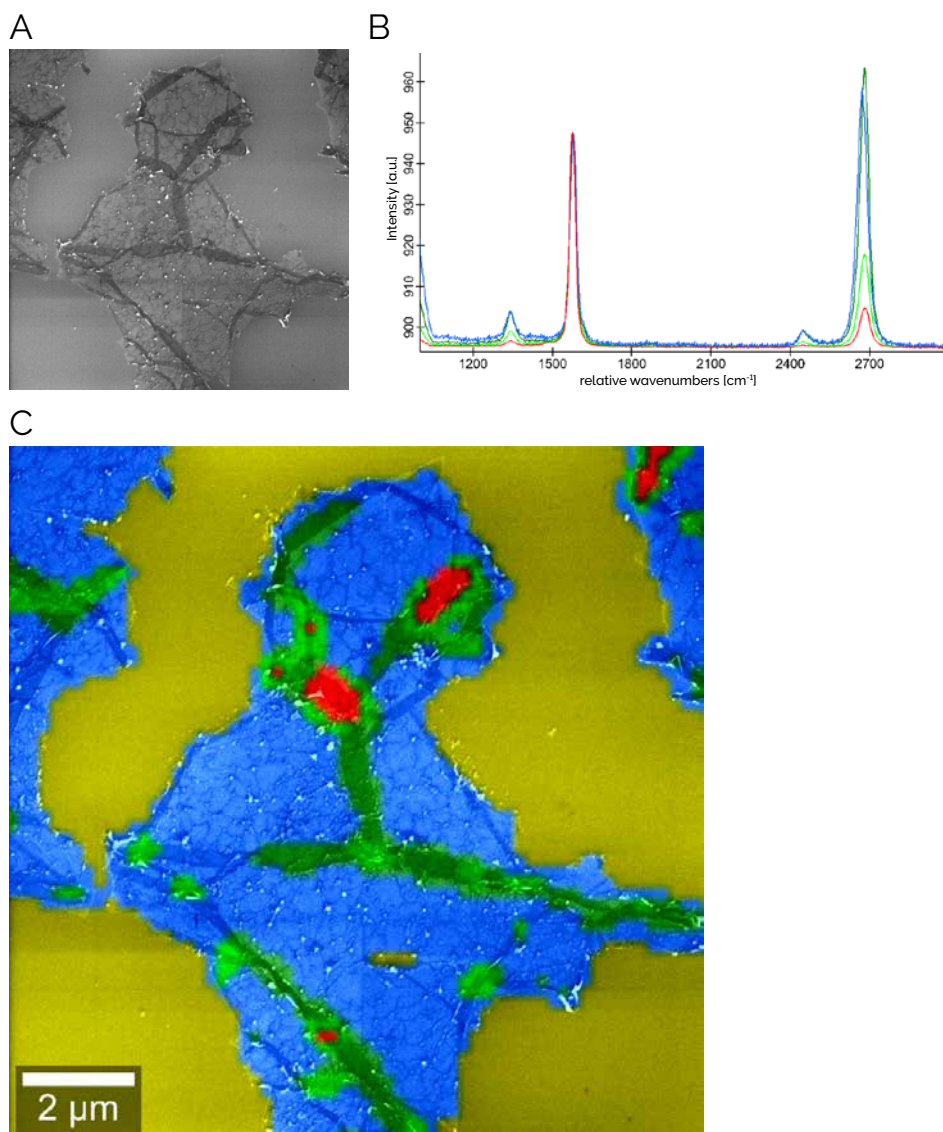
Figure 1: RISE microscopy of graphene.

(A) SEM image of a graphene sample. **(B)** Raman spectra of graphene. **(C)** SEM image overlaid with the color-coded confocal Raman image. The colors display the graphene layers and wrinkles.

Image parameters: 20 x 20 µm², 150 x 150 pixels = 22,500 spectra, integration time: 0.05 s/spectrum, 1 layer (blue, dark green), more than 1 layer (light green, red), Si (yellow).
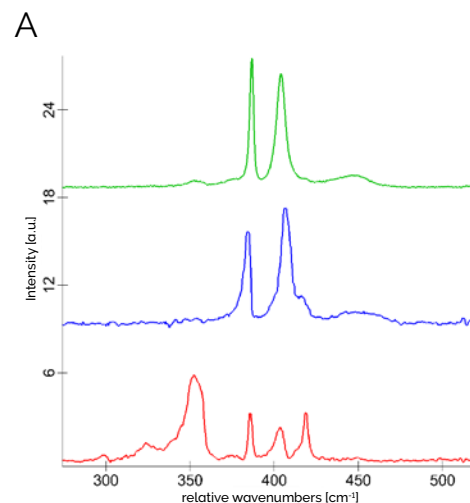
RISE microscopy of MoS$_2$

RISE microscopy reveals the structure as well as the crystalline and exciton dynamics of few-layered transition metal dichalcogenides (TMDs).

CVD-grown monolayers of MoS$_2$ form triangular two-dimensional crystals. Twin crystals of MoS$_2$ on SiO$_2$/Si appear in the SEM image as star-shaped forms (Figure 2B). The Raman spectra of MoS$_2$ monolayers show the characteristic E'/ E$_{2g}$ and A'$_1$/A$_{1g}$ Raman band modes of MoS$_2$ at 385 and 403 relative wavenumbers (cm^{-1}), respectively (Figure 2A). With an increasing number of layers the two Raman bands drift apart due to in-plane and out-of-plane (inter-layer) vibrations.

Here the green spectrum indicates monolayer MoS$_2$ while the blue and red spectra signify edges and defects, respectively.

The spectral information was used to create a Raman image which was overlaid on the SEM image to result in a RISE image (Figure 2C). The grain boundaries visible in the SEM image correlate perfectly with the areas where Raman signals indicate wrinkled or overlapping edges, highlighting the effectiveness of RISE imaging for characterizing MoS$_2$ crystals.
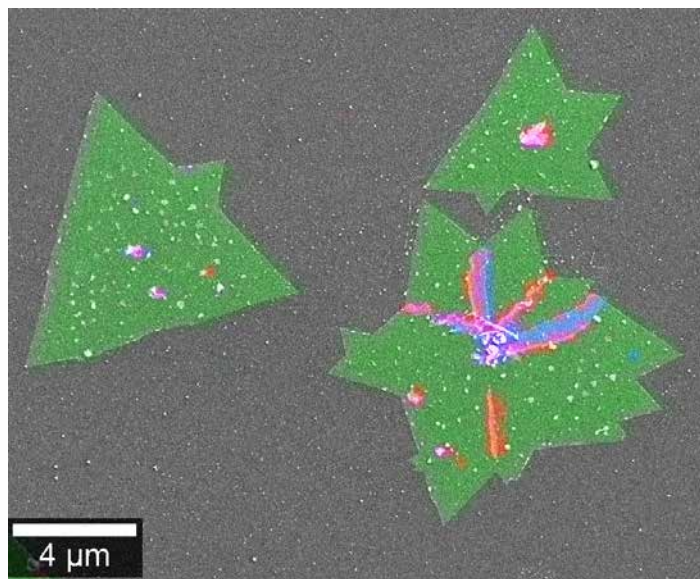
A

B

4 µm

C

4 µm
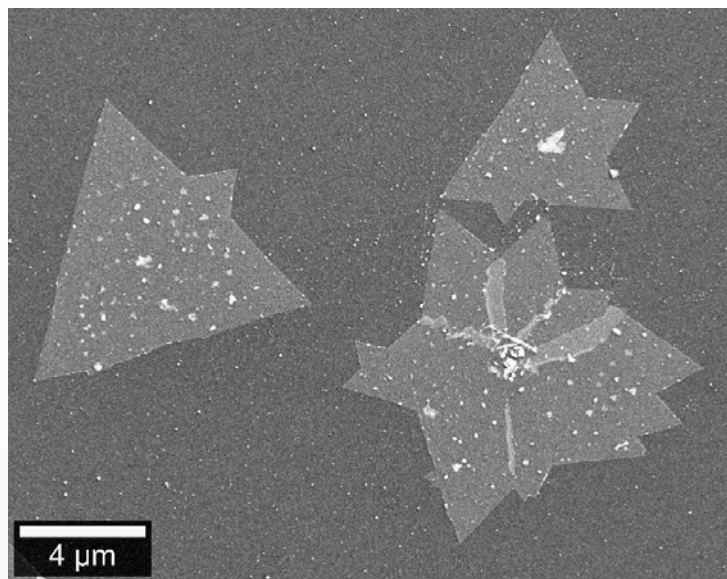
Figure 2: RISE microscopy of MoS$_2$ crystals.

(A) Raman spectra of MoS$_2$: green = 1L MoS$_2$, blue and red = edges and defects. **(B)** SEM image of MoS$_2$ crystals. **(C)** Color-coded Raman image derived from the spectral information overlaid on the SEM image to produce the RISE image.

Sample courtesy of Ting Yu, Nanyang Technological University, Singapore.

Correlative imaging reveals layers and defects of WS$_2$ crystals

WS$_2$ crystals CVD-grown on a Si/SiO$_2$ substrate form triangular islands. Atomic Force Microscopy (AFM) was used to measure their layer thickness (Figure 3A). The flakes are comprised of 1, 2 and more layers. The Raman spectrum of WS$_2$ displays a typical in-plane (E'/E$_g$) mode at 352 relative wavenumbers (cm^{-1}) and an out-of-plane (A'$_1$/A$_{1g}$) mode at 416 relative wavenumbers (cm^{-1}) [1]. The Raman image of the intensity at 416 relative wavenumbers (cm^{-1}) shows that this signal is strongest in those parts of the crystals that consist of two or more layers and defects, respectively (Figure 3B).

The number of layers and the type of layer stacking influences not only Raman peaks' intensities and positions but also the intensity of photoluminescence peaks and their positions. Due to its direct bandgap, monolayer WS$_2$ shows a strong PL signal around 635 nm when excited with a 532 nm laser (Figure 3C). This PL signal decreases significantly with increasing layer numbers because the direct bandgap that is present solely in single-layered TMDs allows for direct recombination of electrons and holes (Figure 3D). Also the PL peak position varies and PL lifetime changes with thickness: the more layers the more PL shifts to the red (Figure 3E) and PL lifetime grows shorter (Figure 3F).

Scanning Near-field Optical Microscopy (SNOM) with down to 60 nm spatial resolution was also used for TMD characterization [2,3]. Here, a strong PL signal indicates edge defects in the material, as shown in a high-resolution SNOM image of another WS$_2$ crystal (Figure 3G). These can also be deduced from PL peak position changes (Figure 3H).
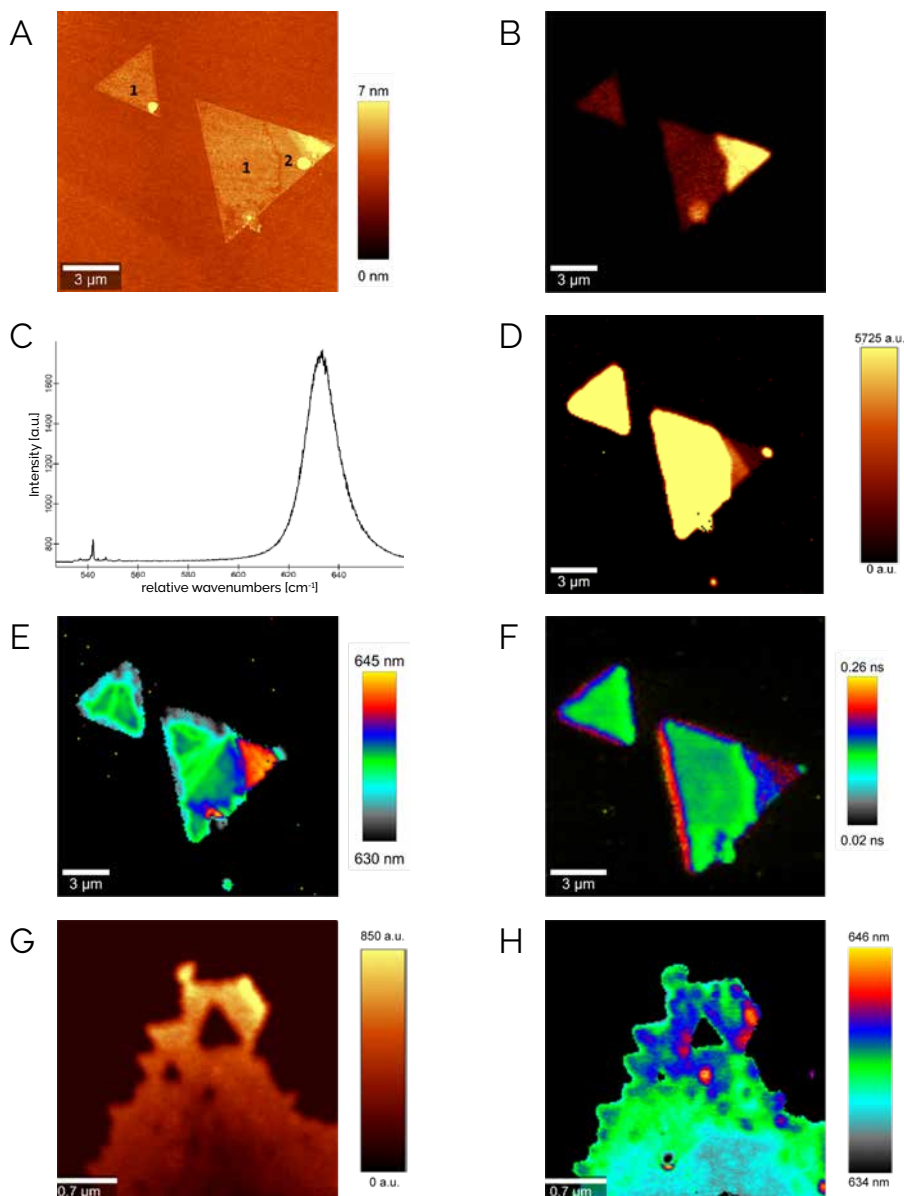
Figure 3: Correlative AFM-SNOM-PL imaging of WS$_2$.
(A) AFM image of CVD-grown WS$_2$ flakes on a Si/SiO$_2$ substrate with varying numbers of layers (1, 2, >2). **(B)** A peak intensity map of the 416 relative wavenumbers (cm^{-1}) Raman mode. **(C)** Upon excitation with a 532 nm laser, WS$_2$ shows a very strong PL signal around 635 nm. **(D)** PL intensity map of the WS$_2$ flakes at 635 nm corresponds exactly to the thickness of the material. **(E)** Position map of PL maxima. **(F)** PL lifetime map. **(G)** A high-resolution SNOM-PL image of a WS$_2$ flake reveals edge defects that correlate with strong PL. **(H)** The edge defects are also visible in the high-resolution SNOM-PL peak position image.

Sample courtesy of Ting Yu, Nanyang Technological University, Singapore.

RISE imaging and in situ modification of WS$_2$

Here we present the analysis and RISE microscopy imaging of a multi-layered WS$_2$ crystal. It shows the typical triangular shape of the material, as well as the heterogeneity of the surface.

A strong WS$_2$ Raman signal was recorded at approximately 350 relative wavenumbers (cm^{-1}) [4]. Researchers were able to divide this peak into three sub-peaks [1]. They associated a signal at 344 relative wavenumbers (cm^{-1}) with the in-plane E' Raman mode. Using this spectral band we generated a Raman intensity map. Overlaying it with the SEM data produced a RISE microscopy image (Figure 4B).

The Raman signals show that this flake is not homogenously layered. It contains 1L layers and areas with more layers and also defects. The Raman image corresponds very well to the structures revealed by SEM.

Figure 4C shows the overlay of the SEM image and an intensity peak map of PL. The WS$_2$ crystal displays strong and homogenous PL at about 640 nm only in the 1L areas due to the direct bandgap in monolayer WS$_2$. Defects seen in the SEM image exhibit PL intensity variations rich in detail. PL intensity corresponds to the intensity of the Raman signal.
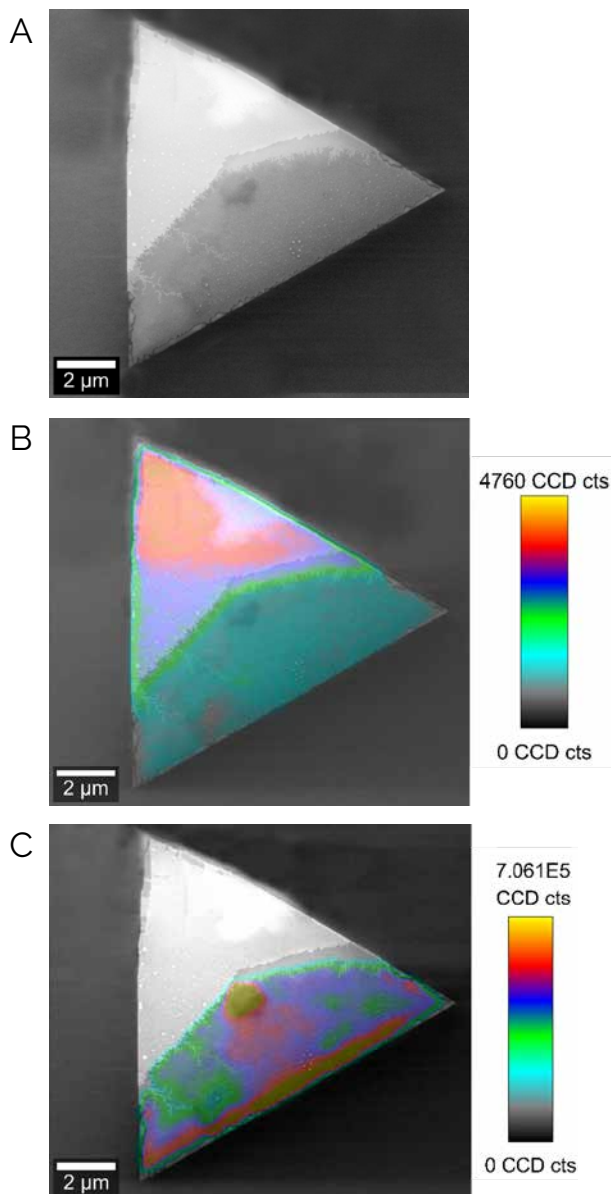

Figure 4: Correlative RISE and SEM-PL microscopy of WS$_2$ crystals.

(A) The SEM image of a WS$_2$ flake reveals defects on the surface and probably adsorbed molecules. **(B)** The correlative RISE microscopy image is composed of the SEM image and the corresponding Raman intensity map over the 344 cm^{-1} Raman band. The Raman image identifies 1L (cyan), 2L (blue) and 3L (red) areas. **(C)** Overlay of the SEM and PL intensity images shows that the 3L area lacks PL (upper part of the triangle). Excitation wavelength for Raman and PL imaging = 532 nm.

Sample courtesy of Ting Yu, Nanyang Technological University, Singapore.

Low-frequency Raman modes and imaging of MoSe$_2$

Not every transition metal dichalcogenide (TMD) can be adequately characterized by its vibrational modes between 200 and 500 relative wavenumbers. In some materials typical in-plane (E'/E$_{2g}$) and out-of-plane (A'/A'1g) modes, though changing in intensity with increasing thickness of the material, do not show peak shifts. Also, these primary Raman peaks are highly sensitive to strain and folding [5] and therefore cannot be used to unambiguously determine the number of layers.

However, low-frequency in-plane shear modes (SM) and out-of-plane layer-breathing modes (LBM) modes are much more informative [6]. To measure Raman spectra close to the laser's excitation wavelength at low wave-numbers between 10 and 50 cm^{-1}, efficient blocking of the Rayleigh line while still transmitting adjacent light is necessary. WITec has developed the RayShield coupler with exactly these features that can be combined with every WITec Raman microscope and is available for 488, 532, 633 and 785 nm lasers.

All measurements of Figure 5 were carried out by Maria O'Brien, Nigel McEvoy and colleagues (Trinity College, Dublin). The low-frequency spectrum shows that 1L MoSe$_2$ has no Raman peak in this range (Figure 5A). With increasing layer numbers SM and LBM peaks occur, shifting in positions and intensities. Accordingly, the flakes that appear to be the thinnest in the optical image (Figure 5B) are almost invisible in the Raman image, whereas thicker material can be detected by their Raman modes (Figure 5C). The type of layer stacking also influences the Raman peaks' intensities and positions. In stable, semiconducting MoSe$_2$ with trigonal prismatic coordination the individual layers can combine in two arrangements, called H and R stacking. These so-called polytypes cannot be distinguished from each other in optical images but can be by their distinctive Raman peaks. Intensity changes in Raman modes at 19 and 24 relative wavenumbers (cm^{-1}) reflect differences in the layer stacking. 2L MoSe$_2$ displays a typical Raman signal at 19 relative wavenumbers (cm^{-1}) that is more intense in the 2H than in the 3R stacking configuration (Figure 5D).

From the peak maximum map at 24 relative wavenumbers (cm^{-1}) it is clear that 3L MoSe$_2$ shows the highest intensity in the 3R3R configuration followed by 2H3R and inverted 3R3R stacking (Figure 5E). O'Brien and colleagues concluded that "... low-frequency Raman mapping can distinguish between different stacking configurations rapidly and non-destructively, allowing TMDs in different stacking configurations to be identified and studied without the need for high-resolution imaging."
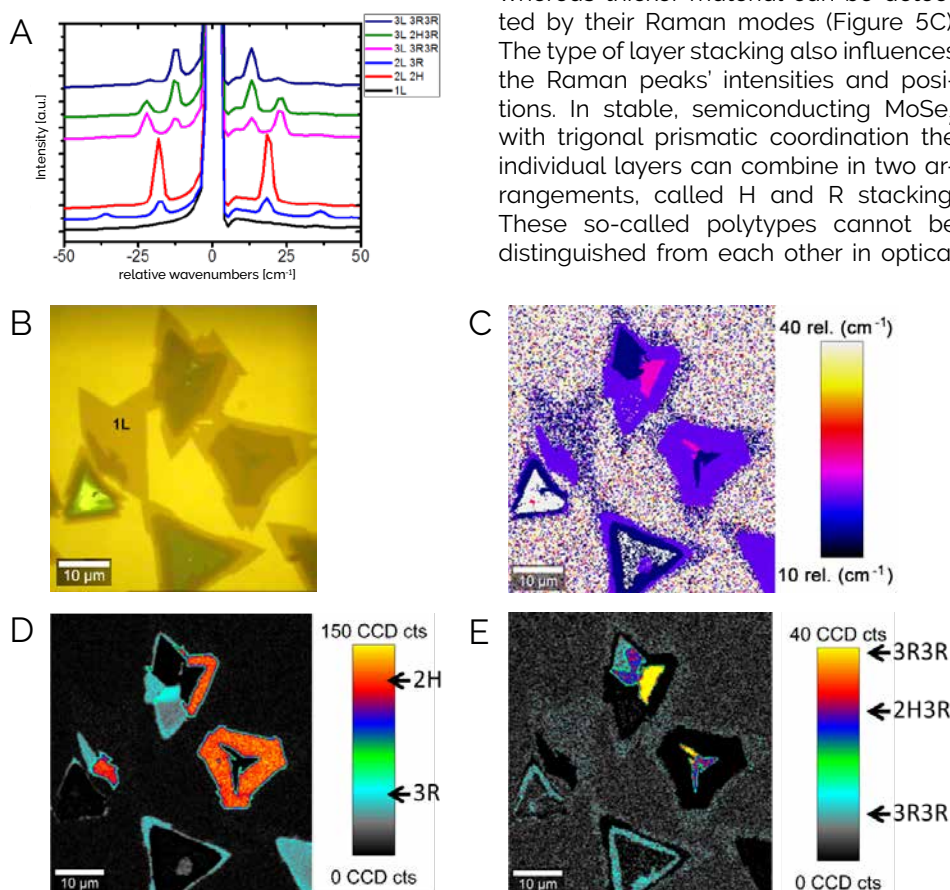

Figure 5: Low-frequency Raman modes of MoSe$_2$.

(A) Low-frequency Raman spectra of 1L, 2L and 3L MoSe$_2$ with various layer configurations (H and R). **(B)** Optical image of CVD-grown MoSe$_2$ reveals differences in thickness and structure of the crystals. **(C)** Map of position of maximum peak intenstiy over the range of 10 to 40 relative wavenumbers (cm^{-1}). **(D)** Peak intensity map of 2L MoSe$_2$ at 19 relative wavenumbers (cm^{-1}). **(E)** Peak intensity map of 3L MoSe$_2$ at 24 relative wavenumbers (cm^{-1}).

Images courtesy of O'Brien, McEvoy and colleagues, Trinity College, Dublin, Ireland.

References

[1] Peimyoo N., et al. (2013). Nonblinking, intense two-dimensional light emitter: monolayer WS2 triangles. *ACS nano*, 7(12), 10985-10994.

[2] Lee, Y., et al. (2015). Characterization of the structural defects in CVD-grown monolayered MoS 2 using near-field photoluminescence imaging. *Nanoscale*, 7(28), 11909-11914.

[3] Lee, Y., et al. (2017). Near-field spectral mapping of individual exciton complexes of monolayer WS2 correlated with local defects and charge population. *Nanoscale*, 9(6), 2272-2278.

[4] Wang, Y., et.al. (2015). Strain-induced direct–indirect bandgap transition and phonon modulation in monolayer WS2. *Nano Research*, 8, 2562-2572.

[5] Zhang, X., et al. (2013). Raman spectroscopy of shear and layer breathing modes in multilayer MoS2. *Physical Review B—Condensed Matter and Materials Physics*, 87(11), 115413.

[6] O'Brien, M., et al. (2016). Mapping of low-frequency Raman modes in CVD-grown transition metal dichalcogenides: Layer number, stacking orientation and resonant effects. *Scientific reports*, 6(1), 19476.

WITec Microscopes

alpha300 S:
Scanning Near-field
Optical Microscope

alpha300 A:
Atomic Force
Microscope

alpha300 R:
Confocal Raman
Microscope

alpha300 R*i*:
Inverted Confocal
Raman Microscope

RISE®: Raman Imaging
and Scanning Electron
Microscope

alpha300 *apyron*™: Automated
Confocal Raman Microscope

alpha300 *access*:
Confocal Micro-Raman System

**Find your regional WITec and Oxford Instruments
contact at https://raman.oxinst.com/contact**